# A simple second-order cartesian scheme for compressible flows

Yannick Gorsse, Angelo Iollo, Lisl Weynans

# A Simple Second Order Cartesian Scheme for Compressible Flows

Y. Gorsse, A. Iollo and L. Weynans

**Abstract** A simple second order scheme for compressible inviscid flows on cartesian meshes is presented. An appropriate Rieman solver is used to impose the impermeability condition. The level set function defines the immersed body and provides some useful geometrical data to increase the scheme accuracy. A modification of the convective fluxes computation for the cells near the solid ensures the boundary condition at second order accuracy. The same procedure is performed in each direction independently. An application to the simulation of a Ringleb flow is presented to demonstrate the accuracy of the method.

**Key words:** compressible flow, second order scheme, level set method, Riemann solver, cartesian meshes
**MSC2010:** 65M08 , 65M12 , 76N15

## 1 Introduction

The computation of flows in complex unsteady geometries is a crucial issue to perform realistic simulations of physical or biological applications like for instance biolocomotion (fish swimming or insect flight), turbomachines, windmills... To this end several class of methods exist. Here we are concerned with immersed boundary methods, i.e., integration schemes where the grid does not fit the geometry. These methods have been widely developed in the last 15 years, though the first methods were designed earlier (see for example [10], [2], [3]). The general idea behind immersed boundary methods is to take into account the boundary conditions by a modification of the equations to solve, either at the continuous level or at the discrete

Y. Gorsse , e-mail: yannick.gorsse@math.u-bordeaux1.fr
A. Iollo , e-mail: angelo.iollo@math.u-bordeaux1.fr
L. Weynans , e-mail: lisl.weynans@math.u-bordeaux1.fr
Institut de Mathematiques de Bordeaux and INRIA Bordeaux Sud-Ouest, Université Bordeaux 1

one, rather than by the use of an adapted mesh. The main advantages of using these approaches, compared to methods using body-conforming grids, are that they are easily parallelizable and allow the use of powerful line-iterative techniques. They also avoid to deal with grid generation and grid adaptation, a prohibitive task when the boundaries are moving. A recent through review of immersed boundary methods is provided by Mittal and Iaccarino [6].

In this paper we present a simple globally second order scheme inspired by ghost cell approaches to solve compressible inviscid flows. In the fluid domain, away from the boundary, we use a classical finite-volume method based on an approximate Riemann solver for the convective fluxes and a centered scheme for the diffusive term. At the cells located on the boundary, we solve an *ad hoc* Riemann problem taking into account the relevant boundary condition for the convective fluxes by an appropriate definition of the contact discontinuity speed. These ideas can be adapted to reach higher order accuracy. However, here our objective is to device a method that can easily be implemented in existing codes and that is suitable for massive parallelization.

In section 2 we describe the finite volume scheme used to solve the flow equations in the fluid domain, away from the interface. In section 3 we introduce our method to impose impermeability condition. Finally, in section 4 we present a numerical test in two dimensions to validate the expected order of convergence and to discuss performance compared to others immersed boundary or body fitted methods.

## 2 Resolution in the fluid domain

We briefly describe how we solve the Euler equations in the fluid domain.

### 2.1 Governing equations

The compressible Euler equations are:

$$\frac{\partial \rho}{\partial t} + \nabla \cdot \rho \mathbf{u} = 0 \tag{1}$$

$$\frac{\partial \rho \mathbf{u}}{\partial t} + \nabla \cdot (\rho \mathbf{u} \otimes \mathbf{u} + p\mathbf{n}) = 0 \tag{2}$$

$$\frac{\partial E}{\partial t} + \nabla \cdot ((E+p)\mathbf{u}) = 0 \tag{3}$$

$$\tag{4}$$

where $E$ denotes the total energy per unit volume. For a perfect gas

$$E = \frac{p}{\gamma - 1} + \frac{1}{2}\rho \mathbf{u}^2 \text{ and } p = \rho R T \tag{5}$$

### 2.2 Discretization

We focus on a two-dimensional setting. Let $i$ and $j$ be integers and consider the rectangular lattice generated by $i$ and $j$, with spacing $h_x$ and $h_y$ in the $x$ and $y$ direction, respectively.

Let $W$ be the conservative variables, $\mathscr{F}^x(W)$, $\mathscr{F}^y(W))$ the convective flux vectors in the $x$ and $y$ directions, respectively. By averaging the governing equations over any cell of the rectangular lattice we have

$$\frac{dW_{i\,j}}{dt}+\frac{1}{h_x}({\mathscr{F}^x}_{i+1/2\,j}-{\mathscr{F}^x}_{i-1/2\,j})+\frac{1}{h_y}({\mathscr{F}^y}_{i\,j+1/2}-{\mathscr{F}^y}_{i\,j-1/2})=0 \tag{6}$$

where $W_{i\,j}$ is the average value of the conservative variables on the cell considered, $\mathscr{F}^x_{i+1/2\,j}$ the average flux in the $x$ direction taken on the right cell side, and similarly for the other sides.

The average convective fluxes at cell interfaces are approximated using the Osher numerical flux function [9].

A second order Runge-Kutta scheme is used for the time integration.

## 3 A second order impermeability condition

For Euler equations, the boundary condition on the interface is the impermeability assumption, i.e., given normal velocity to the boundary (zero for a static wall, but non-zero for a moving solid). We are concerned with recovering second order accuracy on the impermeability condition.

### 3.1 Level set method

In order to improve accuracy at the solid walls crossing the grid cells we need additional geometric information. This information, mainly the distance from the wall and the wall normal, is provided by the distance function. The level set method, introduced by Osher and Sethian [8], is used to implicitly represent the interface of solid in the computational domain. We refer the interested reader to [11], [12] and [7] for recent reviews of this method. The zero isoline of the level set function represents the boundary $\Sigma$ of the immersed body. The level set function is defined by:

$$\varphi(x)=\begin{cases} dist_\Sigma(x) & \text{outside of the solid}\\ -dist_\Sigma(x) & \text{inside of the solid}\end{cases} \tag{7}$$

A useful property of the level set function is:

$$\mathbf{n}(x)=\nabla\varphi(x) \tag{8}$$

where $\mathbf{n}(x)$ is the outward normal vector of the isoline of $\varphi$ passing on $x$. In particular, this allows to compute the values of the normal to the interface, represented by the isoline $\varphi = 0$.

### 3.2 The impermeability condition in one dimension

To make the ideas clear, let us start from a simple case. The typical situation for a grid that does not fit the body is shown in Fig. 1. The plan is to modify the flux at the cell interface nearest to the boundary of the solid, in order to impose the boundary condition at the actual fluid-solid interface location. For a fixed body, we want to impose $u_b = u(x_b) = 0$ at the boundary point $x_b$ where $\varphi(x_b) = 0$.

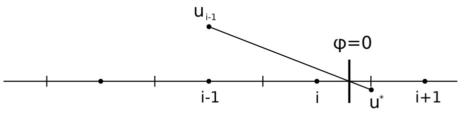

**Fig. 1** Mesh near the solid. The interface lies between the center of cell $i$ (fluid) and the center of cell $i+1$ (solid). The flux in $i+1/2$ has to be modified in order to account for the boundary conditions.

Let $u^*$ be the contact discontinuity speed resulting from the solution of the Riemann problem defined at the interface between cell $i$ and cell $i+1$. The plan is to define a fictitious fluid state in $i+1$ such that the resulting velocity at the interface $u^*$ takes into account, at the desired degree of accuracy, the boundary condition $u_b = 0$ in $x_b$. In particular, taking a second order Taylor expansion of the velocity at $x_b$, we have

$$u^* = u_b + \left(\frac{h_x}{2} - \varphi_i\right) \left.\frac{\partial u}{\partial x}\right|_{x_b} + O(h_x^2) \tag{9}$$

The boundary can be located anywhere between $x_i$ and $x_{i+1}$, so to ensure a well defined derivative (if $x_b \rightarrow x_i$, $\dfrac{u_b - u_i}{x_b - x_i}$ is not numerically well defined), we use $x_{i-1}$ instead of $x_i$ to compute the first order derivative at the interface:

$$\left.\frac{\partial u}{\partial x}\right|_{x_b} = \frac{u_b - u_{i-1}}{h_x + \varphi_i} \tag{10}$$

To obtain $u^*$ as the contact discontinuity speed of the Riemann problem, having computed the left state of the Riemann problem with the MUSCL reconstruction and slope limiters: $U_- = (u_-, p_-, c_-)$, we create the right state $U_+ = (-u_- + 2u^*, p_-, c_-)$, where $c$ is the speed of sound. The left and right state of the variables $p$ and $c$ are chosen identical to express the continuity of these variables on the interface.

### 3.3 The impermeability condition in two dimensions

In two dimensions the flow equations are solved by computing independently the flux in each direction, so we want to apply in each direction the same kind of ideas as in one dimension in order to accurately enforce the boundary conditions. When the level set function changes sign between two cells, we need to modify the fluxes at the interface between these cells.
The interface point is the intersection between the interface ($\varphi = 0$) and the segment connecting the two cell centers concerned by the sign change (for example the points $A$, $B$ and $C$ on Fig. 2). For the flux computation, a fictitious state is created for instance between the cells $(i, j)$ and $(i+1, j)$ on Fig. 2. The boundary condition that we have to impose now is $\mathbf{u}_b.\mathbf{n}_b = 0$, where $\mathbf{u}_b$ is the speed of the fluid at the boundary, and $\mathbf{n}_b$ the outward normal vector of the body.

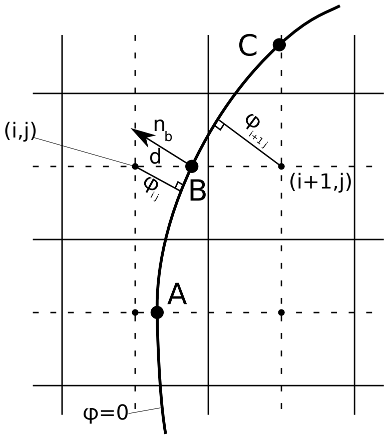

**Fig. 2** Example of geometric configuration at the interface. $B$ is the interface point located between $(i, j)$ and $(i+1, j)$. The flux on cell interface $(i+1/2, j)$ is modified to enforce the boundary condition on $B$.

With reference to Fig. 2, the level set function changes sign between $x_{i,j}$ and $x_{i+1,j}$ at point $B$. Let the normal vector point to the fluid side. If we assume that the boundary $\varphi = 0$ is locally rectilinear, using the side splitter theorem, the distance between $x_{i,j}$ and $B$ is

$$d = \frac{h_x|\varphi_{i,j}|}{|\varphi_{i,j}| + |\varphi_{i+1,j}|} \tag{11}$$

and the normal vector $\mathbf{n}_b$ is computed by

$$\mathbf{n}_b = \mathbf{n}_{i,j} + \frac{d}{h_x}\left(\mathbf{n}_{i+1,j} - \mathbf{n}_{i,j}\right) \tag{12}$$

where $\mathbf{n}_{i,j}$ is a second order centered finite-difference approximation of $\nabla\varphi$ at point $(i, j)$. To impose the boundary condition at the interface point $B$, we determine a value of the contact discontinuity speed $\mathbf{u}^*$, relative to a Riemann problem defined in the direction normal to the cell side through $x_{i+1/2,j}$, consistent at second order

accuracy with $\mathbf{u}_b \cdot \mathbf{n}_b = 0$ in B. Figure 3 illustrates graphically the following steps. Let the normal component of $\mathbf{u}^*$ be $u_n^* = \mathbf{u}^* \cdot \mathbf{n}_b$.
$u_n^*$ is computed with a second order Taylor expansion of the normal velocity at the interface point, that is:

$$u_n^* = \mathbf{u}_b \cdot \mathbf{n} + \left(\frac{h_x}{2} - d\right) \frac{\mathbf{u}_b \cdot \mathbf{n} - \mathbf{u}_{i-1} \cdot \mathbf{n}}{h_x + d} + O(h_x^2). \tag{13}$$

Then, let determine $u_\tau^*$ the tangential component of $\mathbf{u}^*$ by $u_\tau^* = \mathbf{u}^* \cdot \tau_b$, $\tau_b$ being the vector tangential to the interface at point $B$. We use the continuity property of the tangential component of the velocity to define $u_\tau^*$ according to

$$u_\tau^* = \mathbf{u}_- \cdot \tau \tag{14}$$

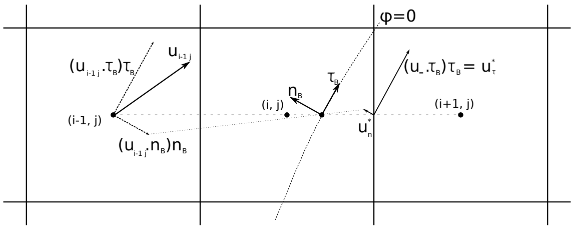
φ=0
$u_{i\text{-}1\,j}$
$(u_{i\text{-}1\,j}.\tau_B)\tau_B$
$(u_{-}.\tau_B)\tau_B = u^*_\tau$
$\tau_B$
$n_B$
(i, j)
(i+1, j)
(i-1, j)
$u^*_n$
$(u_{i\text{-}1\,j}.n_B)n_B$

**Fig. 3** Graphical illustration of the construction of the $\mathbf{u}^*$ vector.

Finally we decompose $\mathbf{u}^*$ in the canonical basis by its horizontal and vertical components $u^*$ and $v^*$, that is

$$u^* = u_n^* n_x + u_\tau^* \tau_x \tag{15}$$

$$v^* = u_n^* n_y + u_\tau^* \tau_y \tag{16}$$

To obtain $\mathbf{u}^*$ as the contact discontinuity speed of the Riemann problem, the left state resulting from the MUSCL reconstruction with slope limiters being $U_- = (u_-, v^*, p_-, c_-)$, we choose the right state to be $U_+ = (-u_- + 2u^*, v^*, p_-, c_-)$.

## 4 Numerical illustration: The Ringleb flow

The objective is to ascertain the actual accuracy obtained at the solid interface.

The Ringleb flow refers to an exact solution of Euler equations. The solution is obtained with the hodograph method, see [13]. The streamlines and iso-Mach lines are shown on Fig. 4.

The exact solution is formulated in $(\theta, V)$ variables with $u = V\cos\theta$, $v = V\sin\theta$ and $V = \sqrt{u^2 + v^2}$.

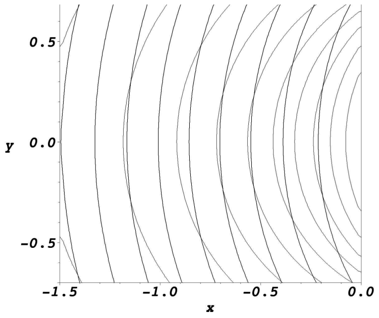

**Fig. 4** Streamlines (black) and iso-Mach lines (grey) of the Ringleb flow.

The stream function is given by $\Psi = \frac{\sin\theta}{V}$.
The streamlines equations are:

$$x = \frac{1}{2\rho}\left(\frac{1}{V^2} - 2\Psi^2\right) + \frac{L}{2}, \quad , \quad y = \frac{\sin\theta\cos\theta}{\rho V^2} \tag{17}$$

with :

$$L = -\left(\frac{1}{2}\ln\frac{1+c}{1-c} - \frac{1}{c} - \frac{1}{3c^3} - \frac{1}{5c^5}\right) \quad , \quad c^2 = 1 - \frac{\gamma-1}{2}V^2 \quad , \quad \rho = c^5 \tag{18}$$

In our test case, the computational domain is $[-0.5;-0.1]\times[-0.6;0]$ and we numerically solve the flow between the streamlines $\Psi_1 = 0.8$ and $\Psi_2 = 0.9$. The inlet and outlet boundary condition are supersonic for $y = -0.6$ and $y = 0$ respectively. The convergence orders are calculated for each variable in $L_1$, $L_2$, $L_\infty$ norms on four different grids 32 × 48, 64 × 96, 128 × 192 and 256 × 384 and presented on table 1.

**Table 1** Global orders of convergence for each variable.

| Variables | $L_1$ norm | $L_2$ norm | $L_\infty$ norm |
|---|---|---|---|
| $x$-velocity | 2.04 | 1.68 | 1.28 |
| $y$-velocity | 1.97 | 1.6 | 1.13 |
| pressure | 2.0 | 2.02 | 1.97 |
| sound velocity | 1.95 | 1.58 | 1.03 |
| entropy | 1.9 | 1.49 | 1.08 |

The error for several variables is order 1 for the $L_{infty}$ norm. Colella et al. [5] obtain the same kind of results on other test cases. One argument developed in [5] to explain this order degradation is that the solid wall is characteristic for entropy, and hence the error on this variable accumulates from inlet to outlet. For the same test case, Coirier and Powell [4] observed also a convergence order between one and two in the case of their own cartesian method. In [1], Abgrall et al. obtain a $L^2$ numerical order of convergence for the density equal to 1.5 with their second order residual distribution scheme.

## 5 Conclusions

In this paper we have presented a new second order cartesian method to solve compressible flows in complex domains. This method is based on a classical finite volume approach, but the values used to compute the fluxes at the cell interfaces near the solid boundary are determined so to satisfy the boundary conditions with a second order accuracy. A test case for inviscid flows was presented. The order of convergence of the method is similar to those observed in the literature. This method is particularly simple to implement, as it doesn't require any special cell reconstruction at the solid-wall interface. The extension to three-dimensional cases is natural as the same procedure at the boundary is repeated in each direction. Forthcoming work will concern the extension of the present approach to multi-physics problems.

## References

1. Abgrall, R., Larat, A., and Ricchiuto, M. Construction of very high order residual distribution schemes for steady inviscid flow problems on hybrid unstructured meshes, in press, 2010.
2. Berger, M., and LeVeque, R. An adaptive cartesian mesh algorithm for the euler equations in arbitrary geometries, 1989.
3. Berger, M., and LeVeque, R. Stable boundary conditions for cartesian grid calculations. *Computing systems in Engineering 1*, 2-4 (1990), 305–311.
4. Coirier, W., and Powell, K. An accuracy assessment of cartesian mesh approaches for the euler equations. *J. Comput. Phys. 117* (1995), 121–131.
5. Colella, P., Graves, D., Keen, B., and Modiano, D. A cartesian grid embedded boundary method for hyperbolic conservation laws. *J. Comput. Phys. 211*, 1 (2006), 347–366.
6. Mittal, R., and Iaccarino, G. Immersed boundary methods, 2005.
7. Osher, S., and Fedkiw, R. *Level Set Methods and Dynamic Implicit Surfaces*. Springer, 2003.
8. Osher, S., and Sethian, J. A. Fronts propagating with curvature-dependent speed: Algorithms based on hamiltonjacobi formulations. *J. Comput. Phys. 79*, 12 (1988).
9. Osher, S., and Soloman, F. Upwind difference schemes for hyperbolic systems of conservation laws. *Math. Comp. 38*, 158 (April 1982), 339–374.
10. Peskin, C. The fluid dynamics of heart valves: experimental, theoretical and computational methods. *Annu. Rev. Fluid Mech. 14* (1981), 235–259.
11. Sethian, J. A. *Level Set Methods and Fast Marching Methods*. Cambridge University Press, Cambridge, UK, 1999.
12. Sethian, J. A. Evolution, implementation, and application of level set and fast marching methods for advancing fronts. *J. Comput. Phys. 169* (2001), 503–555.
13. Shapiro, A. *The Dynamics and Thermodynamics of Compressible Fluid Flow*. Ronald Press, 1953.

The paper is in final form and no similar paper has been or is being submitted elsewhere.